Korean J. Chem. Eng., 36(12), 2085-2094 (2019)
DOI: 10.1007/s11814-019-0402-z

pISSN: 0256-1115
eISSN: 1975-7220

A preferential CO_2 separation using binary phases membrane consisting of Pebax®1657 and [Omim][PF_6] ionic liquid

Kamran Shahrezaei, Reza Abedini†, Mostafa Lashkarbolooki, and Ahmad Rahimpour

Faculty of Chemical Engineering, Babol Noshirvani University of Technology, Babol, Iran
(*Received 2 July 2019 • accepted 10 October 2019*)

Abstract−Pebax®1657 and [Omim][PF_6] ionic liquid (IL) were used to fabricate a blend membrane and applied for CO_2 separation. The changes upon adding ionic liquid into the polymer matrix as well as the membrane characteristics were studied through SEM, FTIR, DSC and TGA analysis. The obtained gas permeation results indicated that the CO_2 permeability in all membranes was much higher than the other studied gases. CO_2 permeability of Pebax containing 8 wt% IL increased from 82.3 Barrer up to 125.6 Barrer at a pressure of 2 bar, which showed a 53% increment compared to the neat Pebax membrane. Furthermore, as the [Omim][PF_6] loading within the polymer matrix was increased, the CO_2/CH_4 and CO_2/N_2 selectivities improved. In addition, the permeability and selectivity of gases was enhanced as the feed pressure increased. Upon increasing feed pressure to 10 bar, the CO_2 permeability of Pebax containing 8 wt% IL reached 185.3 Barrer, which was approximately 48% higher than the permeability at a pressure of 2 bar. Moreover, the selectivity of CO_2/CH_4 and CO_2/N_2 for the Pebax/8 wt% IL membrane at pressure of 2 bar was 15.3 and 46.5, respectively, which improved to 19.7 and 59.8 as the pressure increased to 10 bar.

Keywords: Gas Separation, [Omim][PF_6], Pebax 1657, Permeability, Selectivity

INTRODUCTION

Replacing traditional energy with clean energy has not only gained widespread attention, but due to global warming and climate changes as a result of CO_2 emission, the use of green and renewable energy has drawn remarkable attention. Industries such as natural gas processing, power plants and landfills are the most important sources of CO_2 emission. To deal with mentioned problems, removing CO_2 from process gas streams considered as a potential solution along with environmental regulation to cope with the growing trend of progress in the way of life and economy [1,2].

Developing various gas separation methods with their own advantages and weaknesses is the scope of many studies [3]. In this regard, membrane gas separation processes are considered as emergent and promising, which can be used in different applications, such as ammonia purge gas (H_2/N_2), landfill gas upgrading (CO_2/hydrocarbons), natural gas dehydration (H_2O/hydrocarbons), sour gas treating (H_2S/hydrocarbons) and pre and post-combustion CO_2 capturing. Membrane gas separation has remarkable returns such as application in different process scales, low operational and capital cost, low energy consumption, and low environmental impacts compared to other typical separation processes such as cryogenic, adsorption, and absorption [4,5].

In membrane gas separation processes, productivity is reflected through permeability and selectivity, so that the trade-off, described as "Robeson's upper bound" exists between these two factors [6]. Managing the trade-off between permeability and selectivity in membranes is an important challenge that has restricted the wide application of membrane in industries [7-9]. Generally, membranes that exhibit high permeability along with appropriate selectivity are more attractive to be employed in industrial applications [10].

Among membrane materials, polymers, due to flexibility which is a result of free rotation of segments around main chains, ease of processing and lower cost, have drawn considerable attention particularly in gas separation applications. However, the inappropriate gases selectivity merged with moderate permeability achieved by polymeric membranes has limited these materials to be applied in various gas separation applications. Thus, the type of polymers used to fabricate the membrane can affect the expected performance in all applications [11].

Poly (ether block amid) "Pebax" is a type of elastomeric multiblock copolymer used to prepare gas separation membranes. Pebax consists of poly ethylene oxide (PEO) as a soft segment and polyamide (PA) as a hard semi-crystalline segment [12,13]. Owing to the interaction between PEO segment and polar gases, the permeability would be improved upon the changes in gases' solubility [14-16]. Among different commercial Pebax types, Pebax MH 1657 comprising 40%wt PA segment and 60%wt of PEO one exhibits superior permeability [11,17,18].

Achieving a highly permeable membrane with an appropriate selectivity for gas separation using neat polymeric material is almost impossible. To overcome this restriction and also improve the performance of such membranes, ongoing research has focused on the development of various membranes such as two-component blend membranes and mixed matrix membranes (MMMs) [19].

Ionic liquids (ILs) are one of the candidates to blend with polymers to improve the transport properties of resultant membranes. Mass transport in ionic liquids is generally much faster than poly-

†To whom correspondence should be addressed.
E-mail: abedini@nit.ac.ir

mers [14,20]. ILs' notable features such as high CO_2 adsorption capacity, low volatility and modifiable characteristics have drawn attention in the field of gas separation [21,22]. Thus, an appropriate alternative to overcome the limitations of the ordinary polymeric membranes is blending the polymer matrix with ionic liquids [8,23]. In addition, adding ILs into the polymeric matrix not only enhances the gas permeability, but rather improves the membranes selectivity. ILs based imidazolium, due to an asymmetrical combination of anion and cation in their structures, show high solubility of polar gases like CO_2 compared to light gases such as CH_4 and N_2. In fact, the main reason for the rise in CO_2 solubility which occurs by adding ILs is the interaction between anion part of ILs and gas molecules [15].

Bhattacharya et al. [24] reported the trend of H_2S, CO_2, CH_4 and air permeability though membranes comprising Pebax and [EMIM][$EtSO_4$]. The permeability of H_2S is much higher than that of CO_2 in all membranes. Moreover, in all membranes, the selectivity of H_2S/CO_2 and H_2S/air is much greater than the selectivity of CO_2/CH_4 and CO_2/air.

Mahdavi et al. [8] studied the CO_2 and CH_4 gases permeations through Pebax®1074 blended with [BMIM][PF_6]. They reported that as IL content increased within the polymer matrix, gas permeability was substantially raised from 58.6 to 104.3 Barrer and 2.9 to 5.6 Barrer for CO_2 and CH_4, respectively, while the CO_2/CH_4 selectivity decreased slightly from 20.2 to 18.5.

Fam et al. [25] examined the gas permeation of the Pebax 1657 membrane containing [Emim][BF_4] IL with a thin film composite hollow-fiber structure. Upon increasing of IL to 80% within the polymer network, CO_2 permeability showed a permeability improvement of 70% compared to the pure membrane.

Estahbanati et al. [26] fabricated a two-component membrane containing Pebax1657 polymer and [Bmim][BF_4] for separation of CO_2 from light gases. Through adding IL to the membrane, the gas permeability and corresponding selectivity were improved. Increasing [Bmim][BF4] to 50% resulted in a 73% increment of CO_2 permeability compared to the neat Pebax membrane, and also the CO_2/CH_4 and CO_2/N_2 selectivities were increased by 17% and 34%, respectively.

Hence, based on the results reported, blending the ILs within the polymers is one of the possible alternatives to improve the polar gas permeability and preferential separation of these such gases over the other ones.

Based on some studies about the CO_2 interaction and ILs, the solubility data and also spectroscopic studies reveal that the strong Lewis acid-base interaction between ILs and dissolved CO_2 can affect the CO_2 solubility. Reported results proved that the CO_2-PF_6 interaction is stronger than CO_2-Tf_2N, CO_2-[$N(CN)_2$] [27,28]. The number of carbons of imidazolium cation also affects the permeability of gases. The more carbon number in cationic phase, the higher gas permeability [29]. Thus, in this study, different content of [Omim][PF_6] IL was added into the Pebax 1657 polymeric matrix to improve the gases permeation characteristic of resultant membranes. Fabricated membranes were characterized by means of FTIR and SEM analyses. Thermal properties of membranes were investigated using DSC and TGA analysis. The gas permeation characteristics of membranes were examined at 30 °C and pressure range of 2-10 bar.

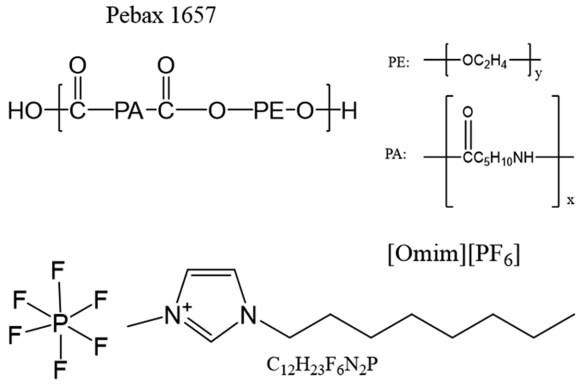

Fig. 1. Chemical structure of Pebax 1657 and [Omim][PF_6].

EXPERIMENTAL STUDY

1. Materials

Pebax®1657 containing 40 wt% PA and 60 wt% PEO in the form of elliptic pellets was purchased from Arkema, France. High purity 3-Methyl-1-octylimidazolium Hexafluorophosphate ([Omim][PF_6]) ionic liquid was purchased from Chemistry and Chemical Engineering Research Institute (CCERI), Iran. Chemical structure of Pebax and [Omim][PF_6] used in this study is shown in Fig. 1. Furthermore, ethanol with a purity of 99.8% (Merck) and deionized water were used and used as a polymer solvent.

2. Membrane Preparation

To prepare a membrane with no defects, one should consider all parameters. Polymer concentration in solution is an important factor which causes a uniform dispersion of IL in the membranes. High concentration of polymer in solution increases solution viscosity and prevents formation of homogeneous and clear solution and leads to thicker and less permeable membranes [26]. In this work, all membranes were fabricated by solution casting. To fabricate neat Pebax membrane, 5 wt% polymer solution was prepared by dissolving Pebax in the mixture of water and ethanol (30 : 70 w/w). The solution vessel was sealed to prevent solvent evaporation and was placed on a magnetic stirrer for 24 hr at uniform temperature of 75-80 °C. To prevent bubble formation and any defect in membrane structure, the polymer solution was kept at stationary for 1 hr at ambient condition. The cast film was allowed for solvent evaporation at ambient temperature for overnight and then it was heated in oven at 50 °C for 6 hr. Finally, fabricated membrane was separated easily from the plate.

The fabrication of Pebax membrane containing [Omim][PF_6] was similar to neat one. After the formation of homogeneous polymer solution, different specific amounts of [Omim][PF_6] were added into the solution and placed on a magnetic stirrer for 3 hr to prevent IL deposition and blended uniformity with Pebax solution. The membrane drying process was the same as the neat Pebax one. Table 1 lists the composition of each casting solution.

3. Membrane Characterization and Performance Evaluation

3-1. Characterization

To characterize intermolecular interactions of pure and Pebax/IL membranes, Fourier transform infrared spectroscopy (FTIR) (TENSOR 27, Brucker Germany) was used in the wave number

Table 1. Composition of the casting solutions for each desired membranes

Membrane	Code	Polymer (5%wt)		Solvent (95%wt)	
		Pebax (%wt)	IL (%wt)	Water (%wt)	EtOH (%wt)
Pure Pebax	P	100	0	30	70
Pebax/2% IL	P-IL2	98	2	30	70
Pebax/4% IL	P-IL4	96	4	30	70
Pebax/6% IL	P-IL6	94	6	30	70
Pebax/8% IL	P-IL8	92	8	30	70

ranges from 400 to 4,000 cm^{-1} under inert conditions.

To investigate the thermal stability of fabricated membranes, thermogravimetric analysis (TGA) method (L81A1550-L81A1750, Linseis Germany) was employed. In this regards, weight-loss is recorded as a function of temperature in controlled atmosphere over a specific time interval. Approximately 20 mg of each membrane was placed in a sample holder and then heated under the rate of 10 °C/min at from 50 to 800 °C.

To analyze the thermal properties of prepared membranes, a 2.3.3. Differential scanning calorimeter (DSC) (PT10, Linseis Germany) was used. Samples of 8-9 mg were heated from −100 to 300 °C with heating rate of 10 °C/min under the nitrogen atmosphere for all samples.

To study the cross-section morphology of neat and blended Pebax/IL membranes, a 2.3.4. scanning electron microscope (SEM) (VEGA-TESCAN) was used.

3-2. Gas Permeation Study

The permeability of CO_2, CH_4 and N_2 through fabricated membranes was measured by constant volume/varying pressure setup. Each gas enters the membrane cell at different upstream pressure, while the permeate gas leaves the cell to be accumulated in the downstream vessel. The rate of pressure change upon gas accumulation was recorded by three calibrated gas pressure sensors with accuracy of 1,000 mbar, 100 mbar and 1 mbar adjusted in series. Gas permeation tests of fabricated membrane were performed at 30 °C and feed pressure of 2 to 10 bar. Gas permeabilities were calculated in terms of Barrer (1 Barrer=1×10^{-10} cm^3 (STP) cm cm^{-2} s^{-1} $cmHg^{-1}$) [22] as follows:

$$P_A = \frac{273.15\times10^{10}VL}{760AT(P_0\times76/14.7)}\frac{dp}{dt} \quad (1)$$

where P_A is permeability of specific gas, T is operational temperature (K), V is constant volume accumulation vessel (cm^3), A is effective membrane area (cm^2), L is membrane thickness (cm), P_0 is feed pressure (psia) and dP/dt is pressure increment in terms of time (mmHg/sec). Ideal selectivity of gases is calculated by Eq. (2):

$$\alpha_{A/B} = \frac{P_A}{P_B} \quad (2)$$

where P_A and P_B are the permeability of gases A and B, respectively [30].

RESULTS AND DISCUSSION

1. Membrane Characterization

1-1. Fourier Transform Infrared Spectroscopy

FTIR analysis of P, P-IL4 and P-IL8 membranes at wave number of 4,000-400 cm^{-1} is shown in Fig. 2. In neat Pebax, several peaks have been reported for specific chemical groups with characteristic bands. Bands at 850 cm^{-1} and 1,122 cm^{-1} are assigned to the symmetric stretching vibration of the C-O-C bond. The PA segment in Pebax polymer has three characteristic peaks, including the amine group, the C=O in bond H-N-C=O, and the stretching vibration of carbonyl (C=O), observed at wave number of 1,546 cm^{-1}, 1,645-1,670 cm^{-1}, 1,739 cm^{-1}, respectively [31,32]. An adsorption band at frequency of 1,400 cm^{-1} relates to the stretching vibration of the C-N in the PA segment. The C-H bond attached to the polymer chain, which shows the symmetrical and non-symmetrical stretching bonding characteristics, is observed at 2,853 cm^{-1} and 2,925 cm^{-1}, respectively. The adsorption bands in the frequency range of 3,050-3,440 cm^{-1} are associated with stretching vibration of the N-H bond in the PA segment, and the band at 3,500 cm^{-1} shows the O-H group stretching bond in the Pebax polymer [25,26,33].

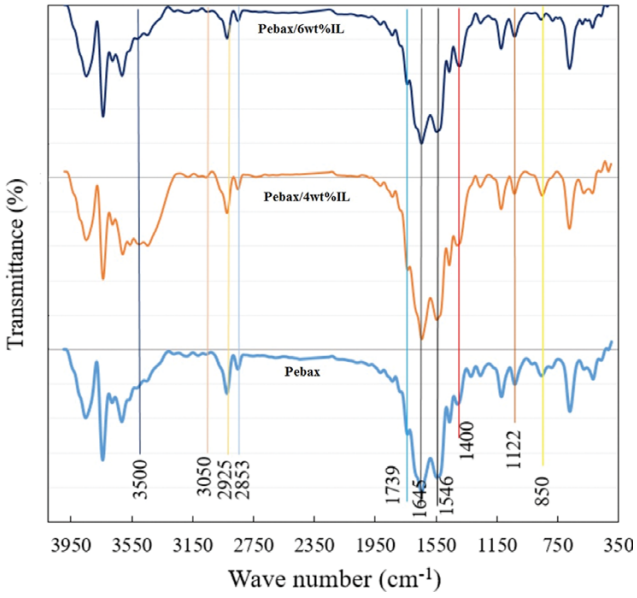

Fig. 2. FT-IR analysis of the neat Pebax, P-IL4 and P-IL8 membranes.

In possible miscible blending materials, there is the probability of interaction between single chains owing to the interaction of a spectrum material, which is an intermediate state between blended and pure one. In general, in FTIR analysis, any change in peak intensity and peak position is due to physical and chemical interactions in the membrane. Through adding IL into the Pebax polymer, the intensity of peak 1,122 cm^{-1} was reduced. This change may indi-

cate that the hydrogen bonding within the molecule is formed between the amine group in [Omim][PF_6] and the oxygen in the PEO segment. By blending the IL into the polymer, the band at 850 cm^{-1} became stronger due to elimination of the intermolecular bond of hydrogen with fluorine atoms [8].

The peak of frequencies 1,546 cm^{-1}, 1,645-1,670 cm^{-1} and 1,739 cm^{-1} was intensified via increasing of IL content, since three groups of amine, the C=O bond and the carbonyl group, in the PA can form hydrogen bonds with IL [26]. The peak at 3,500 cm^{-1} wavelength became broadened upon increasing the IL content and moved toward lower wave number. This change represents an increase in the hydrogen bond between Pebax and IL. Such interactions suggest that Pebax/[Omim][PF_6] combinations are miscible.

1-2. Thermogravimetric Analysis

The synthesized dense membranes were prepared via solvent evaporation, and the final properties of the membrane are affected by the amount of solvent remain in the membrane. The remaining solvent may act as a plasticizer or non-plasticizer agent, and consequently may change the gas separation properties of membranes [34,35]. Hence, to determine if any solvent in the membrane remained or not, the thermal stability of the pure Pebax membrane and the blend membranes containing 2 to 8 wt% IL were determined using thermal gravimetric analysis. Furthermore, the effects of [Omim][PF_6] on thermal stability of Pebax were investigated. The TGA curves for membrane samples are presented in Fig. 3. As can be seen, all membranes show a single stage decomposition, expressing that the presence of IL within the polymer had no significant influence on the thermal degradation pattern of blended membranes. TGA measurements for all membranes include three main steps of remained solvent evaporation, polymeric chain degradation and finally, a carbonization step. The first weight loss step starts at 60 °C and continues to 100 °C for all membranes related to the evaporation of the remaining solvent in the samples. The second stage of weight loss is unique for each sample. Changes start at 300 °C, 245 °C, 240 °C, 235 °C, and 225 °C for P, P-IL2, P-IL4, P-IL6, and P-IL8 membranes, respectively. This weight loss step was due to the Pebax and IL degradation at higher temperature. The degradation temperature of polymer chains in Pebax/IL membranes decreased with the increase of IL content compared to the neat Pebax membrane, which occurs due to the interaction between the polymer and the IL and the polymer chain changes [36].

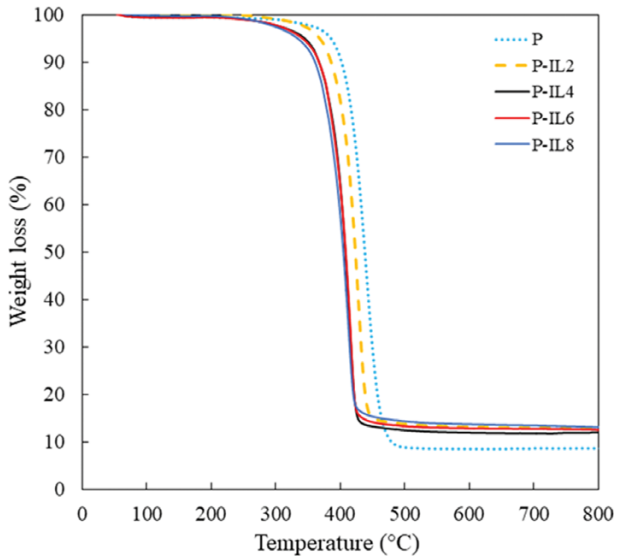

Fig. 3. TGA curves for the neat Pebax and Pebax/IL membranes.

1-3. Differential Scanning Calorimeter

Thermal properties of fabricated membranes were evaluated in terms of measuring the melting point temperature (T_m), glass transition temperature (T_g) and calculation of the degree of crystallinity. In this regards, the double heating scan DSC was proposed to determine the value of T_g exactly [37].

T_g and T_m are a function of the polymer chain mobility and intermolecular interactions, respectively. T_m also depends on the polymer degree of crystallinity and the distribution of the crystal size. The crystallinity degree of soft and hard polymer segments was calculated using Eq. (3) as follow [38]:

$$X_{Crystallinity} = \frac{\Delta H_m}{\Delta H_m^0} \times 100 \quad (3)$$

where ΔH_m is the heat of melting (J/g), determined by dividing the surface area below the melting peaks to the weight of each phase in the sample (60%) PEO and (40%) PA. ΔH_m^0 is the heat of melting of the polymer at 100% crystallinity. The values of ΔH_m^0 for PEO and PA of Pebax 1657 are 166.4 J/g and 233 J/g, respectively [12]. The crystallinity data of all membranes were calculated using Eq. (4) as below:

$$X_{total\ crystallinity} = 0.6X_{PEO,\ crystallinity} + 0.4X_{PA,\ Crystallinity} \quad (4)$$

DSC results for various membranes are presented in Table 2. There are two peaks at 18.5 °C and 208.9 °C, which indicate the melting temperature of PEO and PA phases in the copolymer microphase structure, respectively. The presence of two melting points in the DSC diagrams is in accordance with separate microphase structures in block copolymers. The melting point of the soft phase is less than the melting point of the hard phase. By increasing the amount of [Omim][PF_6], the melting temperature decreases for

Table 2. Results of DSC analysis of Pebax/IL membranes

Sample code	T_g (°C)	$T_{m,PEO}$ (°C)	$T_{m,PA}$ (°C)	$\Delta H_{F,PEO}$ (J/g)	$\Delta H_{F,PA}$ (J/g)	X_{PEO} (%)	X_{PA} (%)	X_{Total} (%)
P	−50.6	18.5	208.9	29.7	77.9	17.9	33.8	24.2
P-IL2	−51.8	19.5	206.9	27.7	74.2	16.6	32.3	22.9
P-IL4	−53.2	13.3	204.1	25.9	73.3	15.6	31.8	22.1
P-IL6	−54.1	15.9	202.8	24.9	69.5	15.0	30.2	21.1
P-IL8	−54.8	12.6	202.8	22.1	65.3	13.2	28.4	19.3

both phases. To provide an explanation, it can be said that IL is an amorphous, low molecular weight polymer, which increases the polymer free volume when loaded to Pebax polymer chain network. So, the crystallinity phase of the membrane decreases and the amorphous phase increases [12,22]. According to Table 2, it can be seen that the crystalline phase of the membranes decreases with increasing IL content in the membrane structure, and the results are in good agreement with similar investigations [12,26]. The [Omim][PF_6] prevents formation of hydrogen bonding in the hard part by placing in the polymer chains, thereby reducing the crystallinity and increasing the permeability of the combined network membrane compared to pure Pebax membranes. Prior to the appearance of the melting peak, some minor peaks are visible in the diagram. These peaks are due to the small amount of crystallinity in the polymer sample, since the material may have a crystalline potential itself and this crystallinity is not yet formed.

T_g temperature values for various types of Pebax were between the −50 and −77 °C, which depends on the molecular weight and the weight distribution of PEO blocks. In this study, at an approximate temperature of 50 °C, there is a smooth peak which is related to the metal transition temperature of the soft copolymer (PEO) section. The glass transition temperature of the hard phase, unlike the soft one, is not detectable by the DSC. Hence, the results are in good agreement with similar studies [14,26,39]. There was only one T_g for each membrane observed in the range of −71 °C and −82 °C. This confirms the assertion that the mixing of IL and Pebax 1657 is homogeneous and does not form two phases [12]. According to Table 2, as the IL within the polymer network increased, the T_g of the membranes decreases.

With regard to the above, the glass transition temperature and partial free volume are somehow related. In this study, the T_g decrement states that adding IL to the polymeric membrane network, increases the amorphous phase, and due to placement in polymer chains can create a gap between the chains, thereby reduction in intermolecular bond strengths.

1-4. Scanning Electron Microscopy

Membrane morphology affects gas permeation properties significantly [17]. Thus, to evaluate the cross-sectional morphology of membranes, SEM analysis was performed. Fig. 4 depicts the high resolution cross-sectional morphology of the neat Pebax and Pebax/IL membranes containing 2 to 8 wt% of [Omim][PF_6]. As can be seen from Fig. 4, all membranes have a thickness between 35 and 45 μm. Fig. 4(a) shows the morphology of a neat Pebax membrane, which has a dense structure with smooth and regular pattern. Referring to Fig. 4(b)-(e), it is clear that, upon adding [Omim][PF_6] into the polymer network, the structure regularity of the membranes decreases and becomes more disordered with a grooved pattern, indicating the proper interaction exists between IL and polymer chains.

Increasing the amount of IL increases the amount of irregularities and converts the structure of the membrane to amorphous. This morphology confirms the results of DSC analysis which proved the crystallinity reduction of membranes as the [Omim][PF_6] content increased in the Pebax matrix. The obtained results of this study are similar to those of other studies related to the addition of low molecular weight materials (i.e., IL) into polymeric membranes [15,26,37].

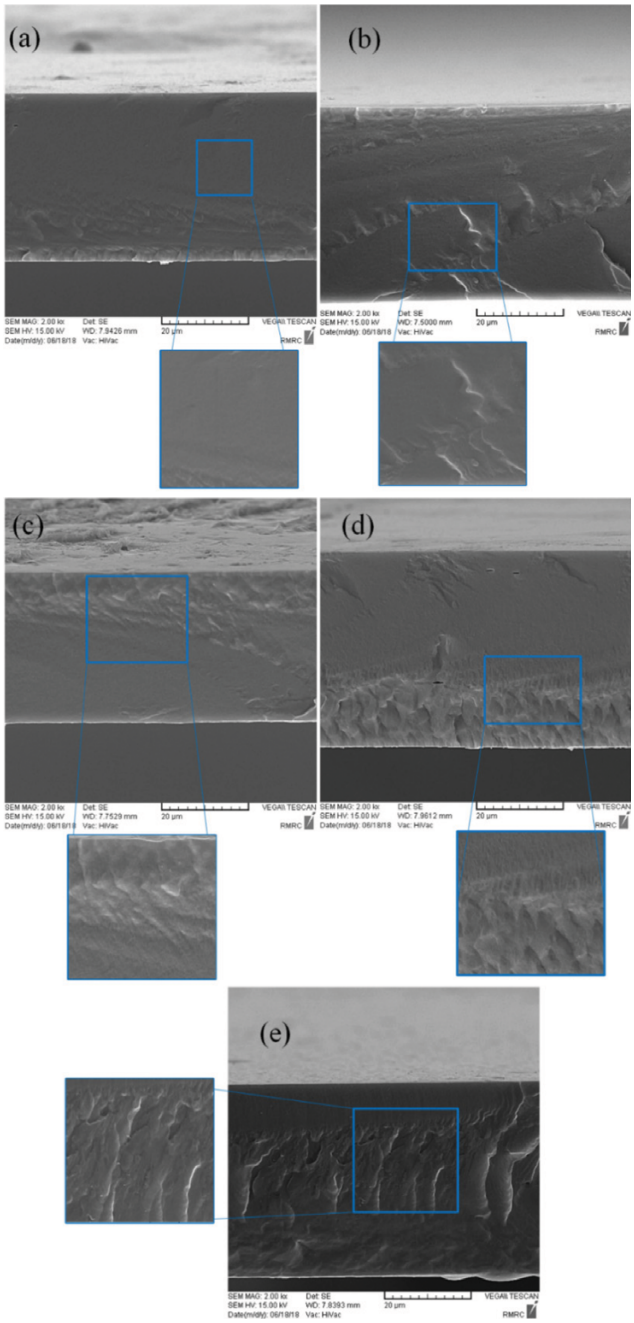

Fig. 4. SEM images of the cross-section morphology of the prepared membranes: (a) neat Pebax, (b) Pebax-IL (2 wt%), (c) Pebax-IL (4 wt%), (d) Pebax-IL (6 wt%) and (e) Pebax-IL (8 wt%) membrane.

2. Gas Separation Performance

A constant volume system was used to measure the permeability and calculate the selectivity of membranes. The permeability of CO_2, CH_4, N_2 and the corresponding ideal selectivity of CO_2/CH_4 and CO_2/N_2, for neat Pebax and Pebax/IL membranes at a temperature of 30 °C and feed pressure of 2 to 10 bars were investigated. Table 3 lists the physical properties of each studied gas.

2-1. The Effect of [Omim][PF_6]

The gas permeability and selectivity values of the neat Pebax

Table 3. Physical properties of gases [38]

Gas	Molecular weight (g/mol)	Kinetic diameter (Å)
CO_2	44.01	3.30
CH_4	16.04	3.80
N_2	28.01	3.64

and Pebax/[Omim][PF_6] membranes at a temperature of 30 °C and a pressure of 2 bar are illustrated in Fig. 5.

As depicted in Fig. 5, CO_2 permeability in all membranes was much higher than CH_4 and N_2. This significant difference is assigned to the high condensability of carbon dioxide compared to other gases and the quadrupole interactions between CO_2 molecules and the PEO segment of Pebax.

This gas separation behavior may be explained by the characteristics of gases such as condensability and the size of the molecules which affect the adsorption of gases by polymer chains. Condensability, which is described by the critical temperature, influences the adsorption of gas in the membrane. More condensable gases show superior adsorption by means of membrane [26]. Additionally, the gas kinetic diameter is another important parameter that controls the gas transport in the membranes. According to Table 3, among all studied gases, CO_2 has a smaller kinetic size, indeed smaller penetrants can pass through the membrane more than larger ones. Besides, carbon dioxide with higher condensability can interact with polymer chains, which improves its permeability. PEO phase has a high tendency to adsorb polar gases such as carbon dioxide. Thus, the PEO segment of Pebax polymer interacts with such polar molecules. CO_2 molecules with four un-bonded joint electron have a quad-dipolar property which interacts with PEO segment of polymer and leads to the improvement of gas sorption within the polymer chains and consequently the CO_2 permeability increases [26]. In fact, the CO_2 solubility can be intensified within the membrane in the presence of CO_2-philic groups (i.e., carbonyl, ether and hydroxyl). CO_2 molecules with positive charged carbon in center can interact with electrons, withdrawing oxygen in PEO and PA of Pebax. This Lewis acid-base interaction can help the CO_2 to transport through the membrane.

For Pebax containing [Omim][PF_6], the gas permeability increased as the IL content increased within the polymer matrix. According to Fig. 5, the permeability of CO_2, CH_4 and N_2 through the P-IL8 membrane increased by 53, 21 and 23%, respectively, compared to the neat Pebax membrane.

Increased gas permeability may also be attributed to the chain mobility. The Pebax 1657 polymer consists of two phases of PA and PEO with individual characteristics. As the [Omim][PF_6] with low molecular weight was blended into the Pebax, the percentage of crystallinity phase in the membrane decreased. Generally, as the membrane crystallinity decreases, the diffusion of penetrant within the membrane facilitates and improves the permeation of gases through the diffusion mechanism [40]. ILs have an integrated amorphous structure. [Omim][PF_6] with liquid state at ambient temperature can easily be placed between polymeric chains, and by increasing the amorphous phase, it will result in the intensification of polymer chain mobility. Thus, the crystallinity of membrane decreases and thereby the free volume of membrane increases. Consequently, the permeability of carbon dioxide, methane and nitrogen gases increases [8].

Additionally, anion has a high effect on the CO_2 permeation in the membranes containing IL [22].

The proper CO_2 solubility in ILs is assigned to the asymmetrical combination of the cation and anion. Hence, as the incompatibility of the ionic parts of the ILs increases, the higher CO_2 solubility could be predicted in the ILs. The physical adsorption mechanism is a result of the interaction between CO_2 molecules and ILs in which the gas molecules occupy the free space in the ILs structure by means of a high quadrupole and van der Waals forces. Further, the Lewis acid-base interaction among the CO_2 and anion of the IL has a significant charge in CO_2 solubility in ILs. Indeed, CO_2 interacts with the anionic part of [Omim][PF_6] (i.e., [PF_6]) and the CO_2 permeation within the polymer increases significantly. Furthermore, due to PEO segment interaction with polar gas molecules, and the limited solubility and diffusion, the permeability im-

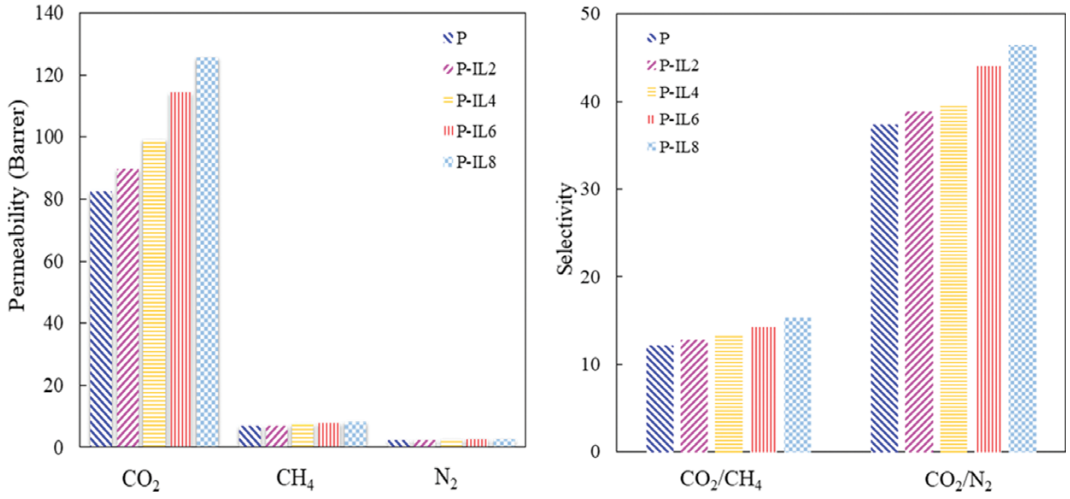

Fig. 5. Effect of [Omim][PF_6] addition on permeation properties of membranes.

provement for other light gases (i.e., methane and nitrogen) is not significant. In fact, as seen from DSC results, the crystallinity of Pebax/IL decreased as the IL content increased; thus the larger gases' (such as methane and nitrogen) diffusivity can be improved to some extent.

The results of the CO_2/CH_4 and CO_2/N_2 selectivities at pressure of 2 bar and temperature of 30 °C for all membranes are shown in Fig. 5. According to the obtained results, it is obvious that CO_2/N_2 selectivity was higher than CO_2/CH_4, because the nitrogen has a much lower permeability than methane in all tested membranes.

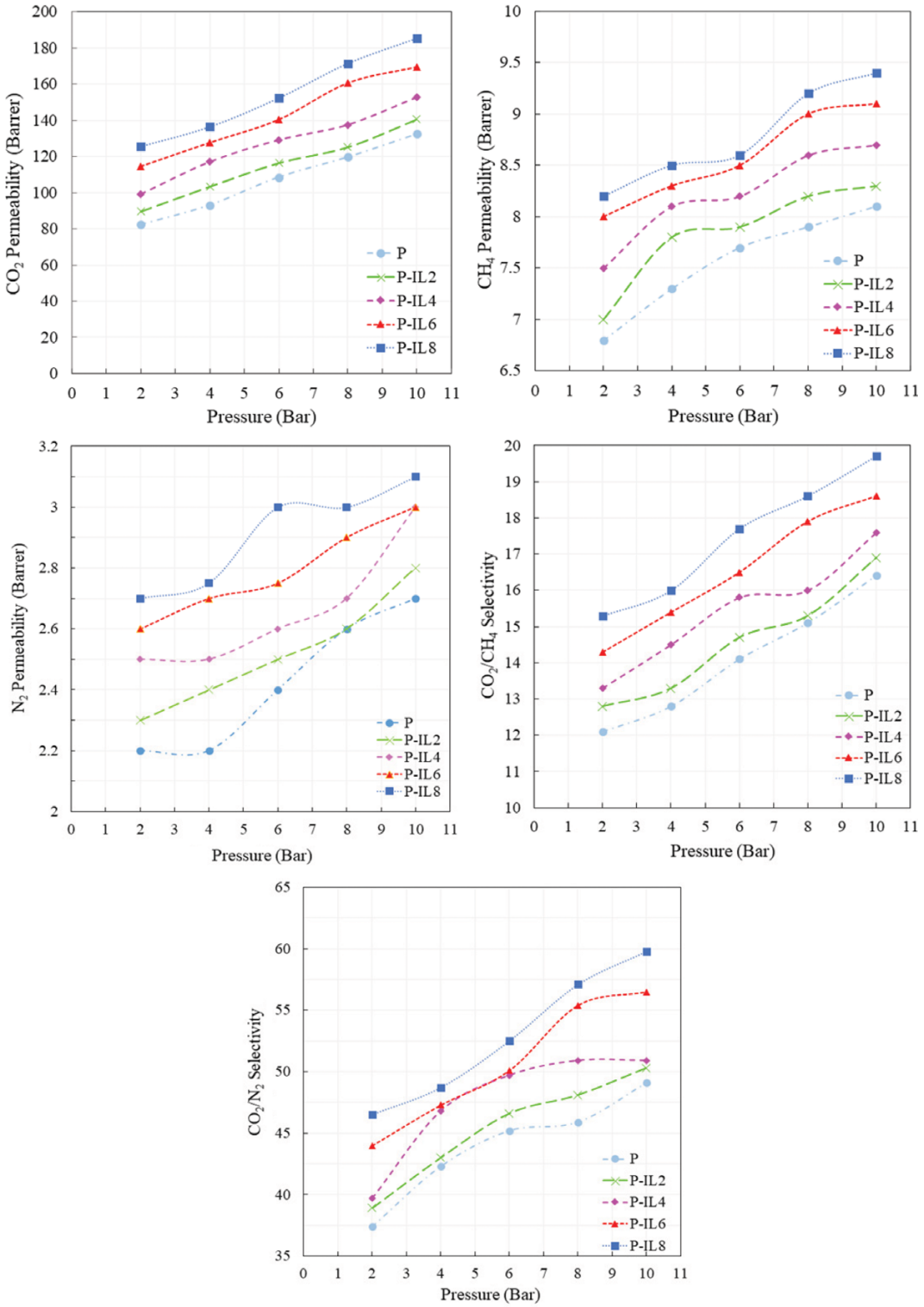

Fig. 6. Effect of pressure on permeation properties of membranes.

Moreover, by increasing the [Omim][PF_6] content within the polymer matrix, the gas pair selectivity is enhanced like gas permeability. For example, the selectivity of CO_2/CH_4 and CO_2/N_2 for neat Pebax membranes was 12.1 and 37.4, respectively, while for P-IL8 membrane, increased to 15.3 (26.5%) and 46.5 (24.5%).

2-2. The Effect of Feed Pressure

Feed gas pressure together with penetrant concentration can affect the properties of membrane gas separation performance. The pressure-dependent permeation of a gases greatly depends on the interaction between the penetrator and the polymer. Many studies have indicated that the permeability of light gases such as hydrogen and nitrogen is nearly independent of pressure, while the permeability of polar and condensable gases through rubbery polymers increases as a result of raising the feed pressure, and conversely, in glassy polymers, gas permeation slowly decreases upon pressure increment. In contrast, the polymer chains compactness along with decreasing the fractional free volume of membrane induced by pressure increment reduces the gas permeation through the membrane. The low penetrant concentration behind the membrane can improve the gas permeation through the membrane, while in the front of the membrane can produce the reverse effect. As the feed pressure increases, the concentration of gases in the membrane rises, and for the case of CO_2 as a polar condensable gas, higher CO_2 concentration results in the plasticization phenomenon, which has an adverse effect on the separation performance of other gases [25,26].

The permeability of CO_2, CH_4 and N_2 through neat Pebax and Pebax/IL membranes containing various [Omim][PF_6] content were studied at feed pressures from 2 to 10 bar and at a temperature of 30 °C. Fig. 6 depicts the feed pressure effect on the CO_2, CH_4 and N_2 gas permeability. The neat Pebax membrane exhibited a relatively high permeability of carbon dioxide due to high condensability and quadrupole interactions between gas molecules and PEO segments of polymer [22]. As shown in Fig. 6, as pressure increased, the carbon dioxide permeability increased in all membranes due to the high adsorption of ether polar bond in PEO segment and high interaction with IL [25].

Generally, increasing the feed pressure can affect the gas permeabilities within the membranes through three main ways [16]:

1. The membrane fractional free volume decreases due to the polymer chains compactness,

2. Increasing the feed pressure improves the driving force for gases to diffuse through the membrane, and therefore, increasing

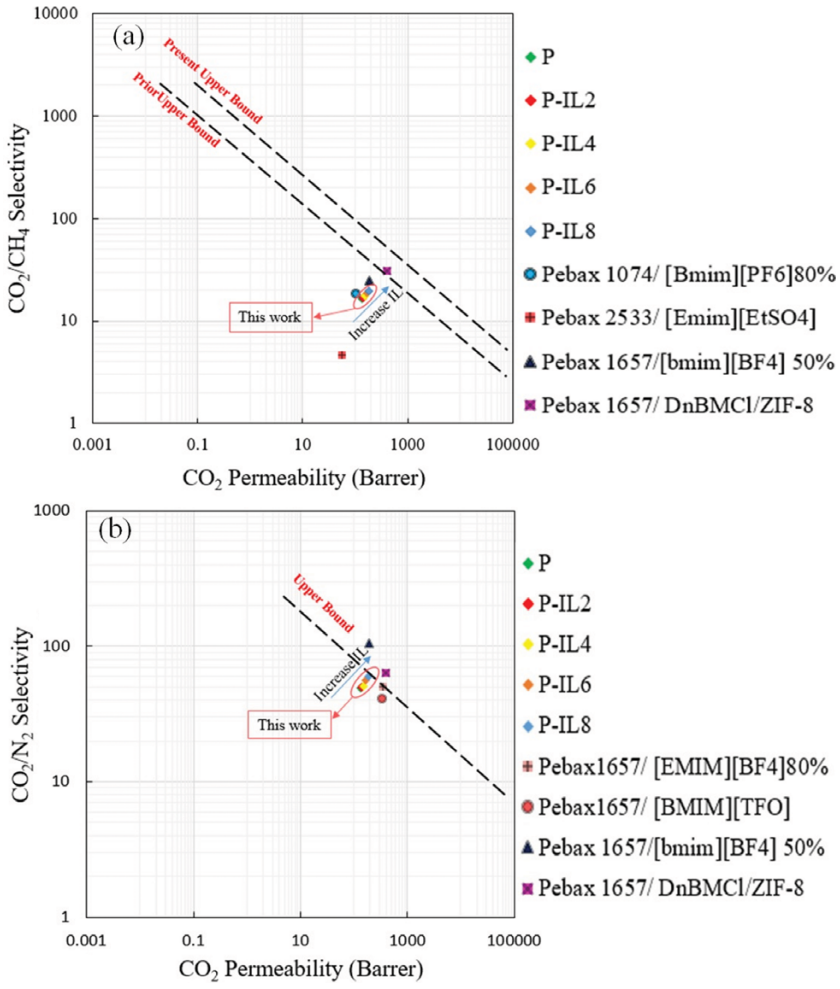

Fig. 7. (a) CO_2/CH_4 selectivity and (b) CO_2/N_2 selectivity versus CO_2 permeability of the neat Pebax and blended membranes in comparison with Robeson upper bound at a pressure of 10 bar and temperature of 30 °C.

the permeability, and

3. Increase in gas concentration (especially polar condensable gas) results in the plasticization effect.

Plasticization effect caused by the greater CO_2 adsorption on the soft polymeric segment of the membrane leads to local movements in polymeric chains, formerly changes the chained package increases the diffusion coefficient and therefore increases the permeability [36]. These phenomena also increase the permeability of other gases and reduce the selectivity of Pebax membranes.

Moreover, the CO_2 molecules interact with the anionic part of IL (i.e., PF_6) which intensifies the CO_2 sorption within the membrane. The anion PF_6 increases gas sorption at high operating pressures [8], and thereby the carbon dioxide permeation increases in membranes at elevated feed pressures. The results of carbon dioxide permeation at various pressures are in good agreement with the results reported by Jomekian [36], Rabiei [12], and Mahdavi [8] for the Pebax 1657/IL membranes.

In this study, the neat Pebax membrane has the lowest carbon dioxide permeation rate among all fabricated membranes. For example, at a pressure of 10 bar, carbon dioxide permeability through the neat membrane was 132.5 Barrer, while increasing to 185.3 Barrer through the P-IL8 membrane, which shows an increase of almost 40%.

In Fig. 6, carbon dioxide selectivity over methane and nitrogen at operating pressure of 2 to 10 bar was reported. As the pressure increases, the selectivity of both cases increases. Regarding the selectivity of 12.1 for CO_2/CH_4 in the neat Pebax membrane at a pressure of 2 bar has the lowest value among all the membranes at all operating pressures, while the P-IL8 membrane with CO_2/CH_4 selectivity of 19.7 exhibited the highest selectivity. In the case of CO_2/N_2 pair, the P-IL8 membrane shows a selectivity of 59.8 at 10 bar, which is approximately 1.6-times greater than the neat Pebax.

2-3. Separation Performance of Membranes

The performance of the neat Pebax membrane and the membranes containing IL in CO_2/CH_4 and CO_2/N_2 separations at 30 °C and 10 bar compared to Robeson bond (2008) is plotted in Fig. 7. The P-IL8 membrane among other fabricated membranes has the best performance in CO_2/CH_4 separation. The performance of the fabricated membranes in the CO_2/N_2 separation is desirable, and the P-IL8 membrane has the best performance among the membranes which lies on the Robson upper bond of the diagram.

The performance of membranes in this work compares to other similar studies reported in Table 4. For the separation of CO_2/CH_4, membranes have a relatively moral performance compared to other works. Furthermore, in the separation of CO_2/N_2 gases, the membranes with good separation performance are located on the upper Robeson bond, and compared to other studies, they indicate a good performance.

CONCLUSION

Membranes based on Pebax 1657 containing various [Omim][PF_6] IL content were fabricated using solvent evaporation. According to SEM analysis, the neat Pebax membrane has a regular and dense structure. By adding IL into the polymer matrix, it progresses to a disordered pattern in the structure, which indicates the appropriate interaction between the polymer and IL. By increasing IL content, the degree of membrane crystallinity was decreased. Measurement of gas permeability showed that, upon adding [Omim][PF_6] into the polymer matrix, the permeability of CO_2, CH_4 and N_2 improved. The addition of [Omim][PF_6] resulted in a significant increase in CO_2 permeability compared to other gases. By increasing in the IL content within the polymer matrix from 0 to 8 wt%, the permeability of CO_2, CH_4 and N_2 increased from 82.5, 6.8 and 2.2, up to 125.6, 8.2 and 2.7 Barrer, respectively. Furthermore, the selectivity of CO_2/CH_4 and CO_2/N_2 was enhanced from 12.1 and 37.4 to 15.3 and 46.5 respectively. The ability of membranes in CO_2/CH_4 and CO_2/N_2 separations was compared to Robson upper bound and the results revealed that the separation performance improved upon adding IL.

ACKNOWLEDGEMENT

The authors acknowledge Babol Noshirvani University of Technology for financial support of this project (Grant NO. BNUT/393054/2018).

REFERENCES

1. R. Lee, Z. Jawad, A. Ahmad and H. Chua, *Process Saf. Environ.*, **117**, 159 (2018).
2. M. H. Nematollahi, S. Babaei and R. Abedini, *Korean J. Chem. Eng.*, **36**, 763 (2019).
3. I. Shakeel, A. Hussain and S. Farrukh, *J. Polym. Environ.*, **27**, 1449 (2019).
4. R. Heck, M. S. Qahtani, G. O. Yahaya, I. Tanis, D. Brown, A. A. Bahamdan, A. W. Ameen, M. Vaidya, J.-P. Ballaguet and R. Alhajry, *Sep. Purif. Technol.*, **173**, 183 (2017).
5. R. Abedini, M. Omidkhah and F. Dorosti, *RSC Adv.*, **4**, 36522 (2014).
6. A. D. Kiadehi, A. Rahimpour, M. Jahanshahi and A. A. Ghorey-

Table 4. A comparison of gas separation performance for Pebax/IL membranes in this work and other similar studies

Membrane	T (°C)	P (bar)	P_{CO2} (Barrer)	CO_2/CH_4	CO_2/N_2	Ref.
Pebax 1074/80% [Bmim][PF_6]	25	2	104.26	18.5	---	[8]
Pebax1657/80% [EMIM][BF_4]	25	12	378.2	18.6	50.0	[12]
Pebax1657/20% [BMIM][TFO]	25	10	87.7	22.4	49.2	[14]
Pebax 2533/[Emim][$EtSO_4$]	30	7	55	4.6	---	[24]
Pebax 1657/50% [BMIM][BF_4]	35	10	188.6	25.1	108.3	[26]
Pebax 1657/8% [Omim][PF_6]	30	10	185.3	19.7	59.8	This work

shi, *J. Ind. Eng. Chem*., **22**, 199 (2015).
7. E. Nezhadmoghadam, M. Pouafshari Chenar, M. Omidkhah, A. Nezhadmoghadam and R. Abedini, *Korean J. Chem. Eng*., **35**, 526 (2019).
8. H. R. Mahdavi, N. Azizi, M. Arzani and T. Mohammadi, *J. Nat. Gas. Sci. Eng*., **46**, 275 (2017).
9. A. Raza, S. Farrukh and A. Hussain, *J. Polym. Environ*., **25**, 46 (2017).
10. L. Hao, P. Li, T. Yang and T.-S. Chung, *J. Membr. Sci*., **436**, 221 (2013).
11. F. Dorosti, M. Omidkhah and R. Abedini, *Chem. Eng. Res. Des*., **92**, 2439 (2014).
12. H. Rabiee, A. Ghadimi and T. Mohammadi, *J. Membr. Sci*., **476**, 286 (2015).
13. M. Vatani, A. Raisi and G. Pazuki, *J. Mol. Liq*., **277**, 471 (2019).
14. P. Bernardo, J. C. Jansen, F. Bazzarelli, F. Tasselli, A. Fuoco, K. Friess, P. Izák, V. Jarmarová, M. Kačírková and G. Clarizia, *Sep. Purif. Technol*., **97**, 73 (2012).
15. E. Ghasemi Estahbanati, M. Omidkhah and A. Ebadi Amooghin, *ACS. Appl. Mater. Inter*., **9**, 10094 (2017).
16. M. Mozafari, R. Abedini and A. Rahimpour, *J. Mater. Chem. A*., **6**, 12380 (2018).
17. H. Hosseinzadeh Beiragh, M. Omidkhah, R. Abedini, T. Khosravi and S. Pakseresht, *Asia-Pac. J. Chem. Eng*., **11**, 522 (2016).
18. M. Pazirofteh, M. Dehghani, S. Niazi, A. H. Mohammadi and M. Asghari, *J. Mol. Liq*., **241**, 646 (2017).
19. T.-S. Chung, L. Y. Jiang, Y. Li and S. Kulprathipanja, *Prog. Poly. Sci*., **32**, 483 (2007).
20. B. Sasikumar, G. Arthanareeswaran and A. Ismail, *J. Mol. Liq*., **266**, 330 (2018).
21. Y. Zhao, M. Pan, X. Kang, W. Tu, H. Gao and X. Zhang, *Chem. Eng. Sci*., **189**, 43 (2018).
22. M. Li, X. Zhang, S. Zeng, H. Gao, J. Deng, Q. Yang and S. Zhang, *RSC Adv*., **7**, 6422 (2017).
23. A. Car, C. Stropnik, W. Yave and K.-V. Peinemann, *Sep. Purif. Technol*., **62**, 110 (2008).
24. M. Bhattacharya and M. K. Mandal, *J. Clean. Prod*., **156**, 174 (2017).
25. W. Fam, J. Mansouri, H. Li and V. Chen, *J. Membr. Sci*., **537**, 54 (2017).
26. E. G. Estahbanati, M. Omidkhah and A. E. Amooghin, *J. Ind. Eng. Chem*., **51**, 77 (2017).
27. M. Bhattacharya and M. K. Mandal, *J. Clean. Prod*., **156**, 174 (2017).
28. R. Lin, L. Ge, H. Diao, V. Rudolph and Z. Zhu, *ACS Appl. Mater. Interfaces*, **46**, 32041 (2016).
29. K. V. Otvagina, A. E. Mochalova, T. S. Sazanova, A. N. Petukhov, A. A. Moskvichev, A. V. Vorotyntsev, C. A. M. Afonso and I. V. Vorotyntsev, *Membranes*, **6**, 31 (2016).
30. N. Azizi, T. Mohammadi and R. M. Behbahani, *J. Energy Chem*., **26**, 454 (2017).
31. R. Abedini, M. Omidkhah and F. Dorosti, *Int. J. Hydrogen Energy*, **39**, 7897 (2014).
32. M. Jamshidi, V. Pirouzfar, R. Abedini and M. Z. Pedram, *Korean J. Chem. Eng*., **34**, 829 (2017).
33. G. Huang, A. P. Isfahani, A. Muchtar, K. Sakurai, B. B. Shrestha, D. Qin, D. Yamaguchi, E. Sivaniah and B. Ghalei, *J. Membr. Sci*., **565**, 370 (2018).
34. Y.-J. Fu, C.-C. Hu, H.-z. Qui, K.-R. Lee and J.-Y. Lai, *Sep. Purif. Technol*., **62**, 175 (2008).
35. C. Joly, D. Le Cerf, C. Chappey, D. Langevin and G. Muller, *Sep. Purif. Technol*., **16**, 47 (1999).
36. A. Jomekian, B. Bazooyar, R. M. Behbahani, T. Mohammadi and A. Kargari, *J. Membr. Sci*., **524**, 652 (2017).
37. R. Nasir, N. N. R. Ahmad, H. Mukhtar and D. F. Mohshim, *J. Environ. Chem. Eng*., **6**, 2363 (2018).
38. E. Parodi, L. Govaert and G. Peters, *Thermochim. Acta*, **657**, 110 (2017).
39. A. Ghadimi, M. Amirilargani, T. Mohammadi, N. Kasiri and B. Sadatnia, *J. Membr. Sci*., **458**, 14 (2014).
40. H. Sanaeepur, R. Ahmadi, A. E. Amooghin and D. Ghanbari, *J. Membr. Sci*., **573**, 234 (2019).